Electronic Supplementary Material (ESI) for Journal of Materials Chemistry C.

Supporting Information

One-step conversion of $CsPbBr_3$ into $Cs_4PbBr_6/CsPbBr_3@Ta_2O_5$ core−shell microcrystals with enhanced stability and photoluminescence

Manli Zhang,[ab] *Yao Li,*[ab] *Kaimin Du,*[ab] *Xuan Gao,*[ab] *Yu Lu,*[a] *Ding Wen,*[ab] *Shuang Yao,*[a] *Jing Feng**[ab] *and Hongjie Zhang**[ac]

[a] State Key Laboratory of Rare Earth Resource, Utilization Changchun Institute of Applied Chemistry, Chinese Academy of Sciences, Changchun 130022, China

[b] University of Science and Technology of China, Hefei 230026, China

[c] Department of Chemistry, Tsinghua University, Beijing 100084, China

* Corresponding authors. Tel.:+86 431 85262127; fax: +86 431 85698041.

E-mail addresses: fengj@ciac.ac.cn (J. Feng), hongjie@ciac.ac.cn (H. Zhang).

Experimental section

Materials: CsBr (≥ 99.9%), and $PbBr_2$ (≥ 99.9%) were purchased from Aladdin. Tantalum (V) ethoxide (TTEO, 99.999%) was purchased from Alfa Aesar. Hexane (99.5%), DMF (99.5%), and Toluene (99.95%) were purchased from Beijing Chemical Reagent Co., Ltd. China.

Preparation of precursor DMF solution: $PbBr_2$ (0.1468 g), CsBr (0.0851g), OAm (0.6 mL), and OA (1.8 mL) were added in 10 mL of DMF. The mixture was then stirred at 90 °C for 2 h to obtain a clear solution.

Synthesis of $Cs_4PbBr_6/CsPbBr_3$ by LASR method: $CsPbBr_3$ could be obtained by adding 0.5 mL of the precursor solution into dry toluene under vigorous stirring. When the mount of DMF solution was increased from 0.5 to 5 mL, $CsPbBr_3$ could transform to Cs_4PbBr_6 gradually. Then, the products were collected by centrifuging at 8000 rpm for 5 minutes.

Synthesis of $Cs_4PbBr_6/CsPbBr_3@Ta_2O_5$ MCs by sol-gel method: Firstly, 0.5 mL of the precursor solution was quickly added into dry toluene under vigorous stirring. After stirring for a while, different amounts of Ta precursor were added into the above $CsPbBr_3$ solution under stirring. Then, the system was then kept stirring under ambient condition. The products were collected by centrifuging at 8000 rpm for 5 minutes.

Fabrication and package test of LED devices: White LED was constructed by employing the as-prepared green powder and red $CdSe_2$ commercial powder on a commercially available a 395 nm blue InGaN LED chip. The chip was first fixed on the bottom of a reflector. Then, as-prepared green powders and red $CdSe_2$ commercial powders were mixed with silicone thoroughly to form a composite sol. The mixture was dropped onto a blue InGaN blue-emitting chip. The optical properties of the fabricated devices were evaluated by using an integrating sphere with an analyzer system (tarspec SSP6612.)

Characterization: The powder X-ray diffraction (XRD) patterns were recorded on a Bruker D8 Focus powder X-ray diffractometer using Cu Kα radiation (λ = 1 .5418 Å) and operating at a voltage of 40 kV and a current of 40 mA. The 2θ angle of the spectra was obtained at a scanning rate of 5°/min. Transmission electron microscopy (TEM), high angle annular dark-field scanning TEM (HAADFSTEM), the elemental 2D-mapping measurements were carried out on a FEI Tecnai G2S-Twin instrument with a field emission gun operating at 200 kV. UV-visible absorption spectra were obtained using a Shimadzu 3600 UV-vis spectrophotometer. The PL spectra were collected on an Edinburgh Instruments FLSP-920 fluorescence spectrometer equipped with a 450 W xenon lamp as the excitation source at room temperature. The temperature-dependent PL spectra were measured by fluorescence spectrometer equipped with a xenon lamp as the excitation source (Edinburgh Instruments FLSP-920) and a temperature controller (INSTEC temperature controller, American Instec). The fluorescent decay curves were obtained from a Lecroy Wave Runner 6100 Digital Oscilloscope (1 GHz) taking a tunable laser (pulse width = 4 ns, gate = 500 ns) as the excitation (Contimuum Sunlite OPO) source. The measured PL decay curves were fitted with a bi-exponential decay function, as expressed $I(t) = a_1 e^{-t/\tau 1} + a_2 e^{-t/\tau 2}$. The average PL lifetime could be calculated by using $\tau_{avg} = \frac{(a_1\tau_1^2 + a_2\tau_2^2)/(a_1\tau_1 + a_2\tau_2)}{a_1 t_1 + a_2 t_2}$. The PLQYs were gained directly by the absolute PL quantum yield measurement system (C9920-02, Hamamatsu Photonics K. K., Japan).

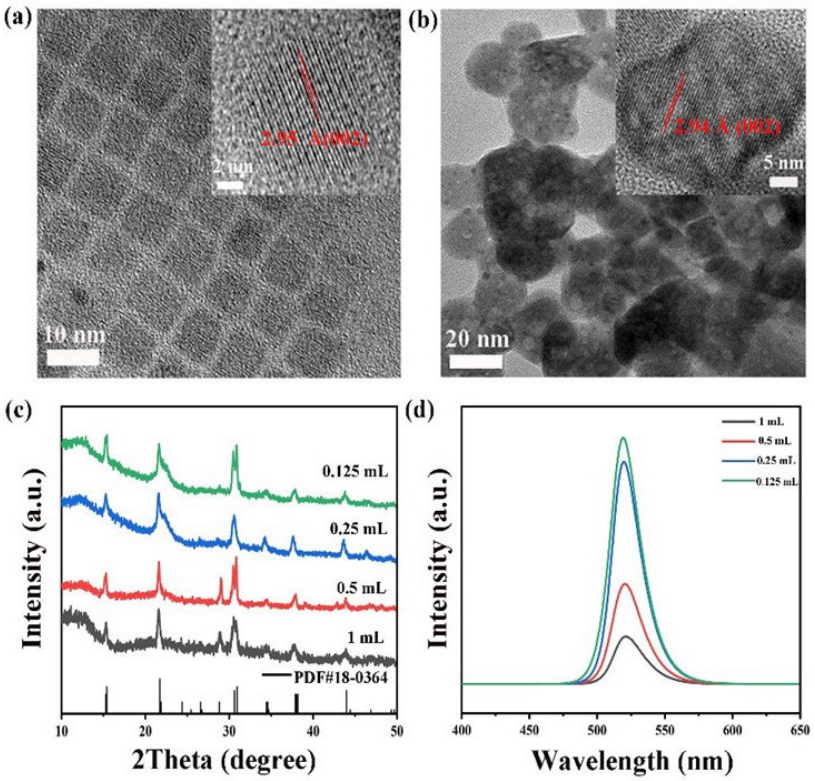

Fig. S1 TEM images of $CsPbBr_3$ with different amounts of DMF precursor solution (a) 0.125 mL and (b) 0.5 mL (Inset: the corresponding HRTEM images), (c) XRD patterns and (d) PL spectra of $CsPbBr_3$ with different amounts of DMF precursor solution, as indicated on the frames.

Table S1. The EDS results of the perovskite crystals samples with different amounts of DMF solution.

Volume of DMF solution	Cs (At%)	Pb (At%)	Br (At%)
1 mL	20.37	19.85	59.78
2 mL	24.14	17.81	58.05
3 mL	27.65	14.66	57.69
4 mL	31.63	11.48	56.89
5 mL	36.10	10.15	53.75
6 mL	36.43	9.88	53.69

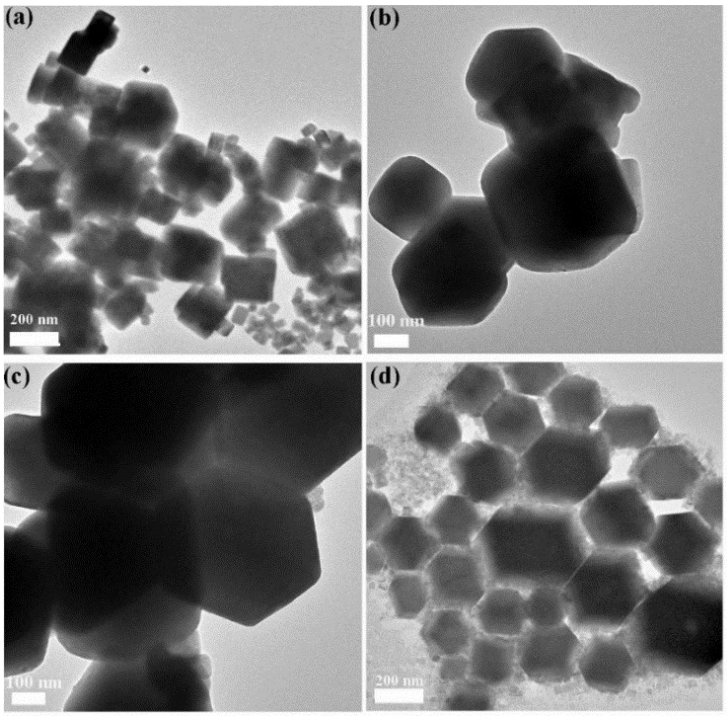

Fig. S2 TEM images of $Cs_4PbBr_6/CsPbBr_3$ with different amounts of DMF solution: (a) 2 mL, (b) 3 mL, (c) 4 mL, and (d) 6 mL.

Table S2. PL Lifetime for Janus $Cs_4PbBr_6/CsPbBr_3$ microcrystals with different amounts of DMF solution (PL lifetime is Fitted by a Biexponential Decay Function)

DMF (mL)	τ_1 (ns)	τ_2 (ns)	A1	A2	τ_{Avg} (ns)	PLQY (%)	Knr
1	2.84	12.53	7.38E+9	151237.1	2.84	2.1	0.34385
2	1.63	9.02	31039.02	8958.99	8.26	22	0.09434
3	4.14	22.14	2289.07	676.96	20.25	39.6	0.02983
4	4.56	24.20	1975.63	910.06	22.79	66.7	0.01461
5	5.19	28.74	2073.96	902.72	27.09	91.5	0.00314
6	4.33	22.83	1994.52	985.79	21.57	74.7	0.01172

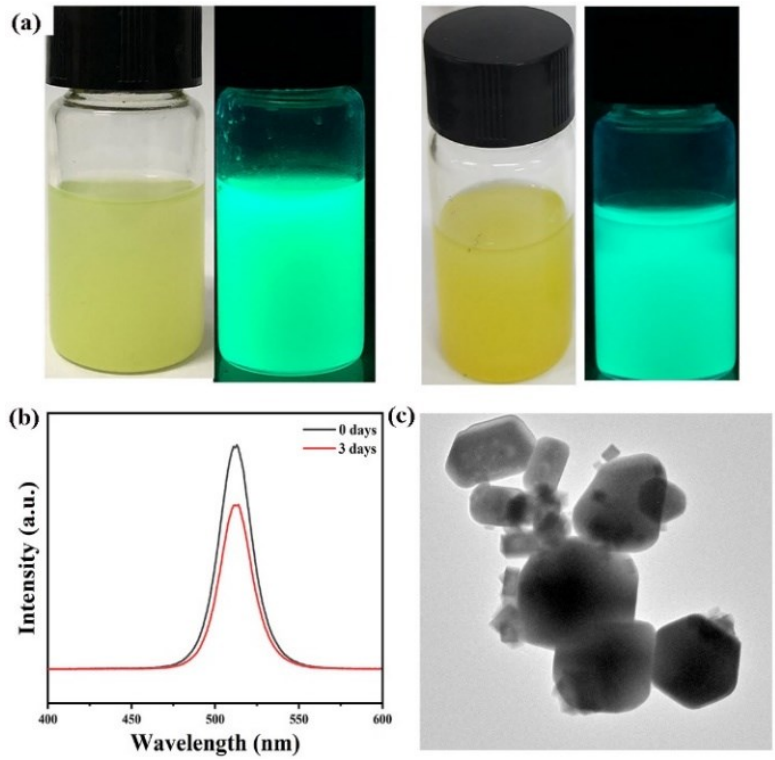

Fig. S3 (a) Photographs of $Cs_4PbBr_6/CsPbBr_3$ under day light and 365 nm UV light (left: 0 day; right: left for 7 days), (b) PL spectra of $Cs_4PbBr_6/CsPbBr_3$, (c) TEM of $Cs_4PbBr_6/CsPbBr_3$ left for 7 days.

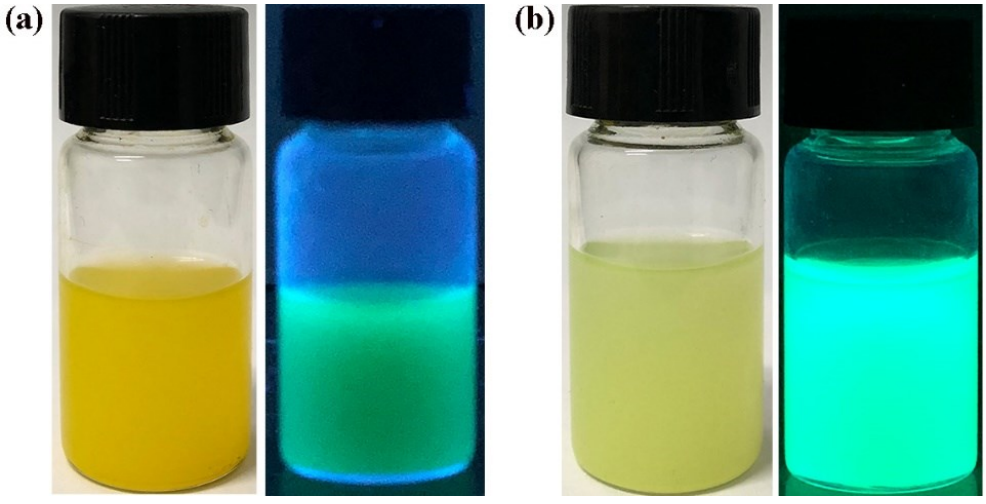

Fig. S4 (a) Photographs of $CsPbBr_3$ under day light (left) and 365 nm UV light (right), (b) Photographs of Cs_4PbBr_6 after adding Ta precursor into $CsPbBr_3$ solution under day light (left) and 365 nm UV light (right).

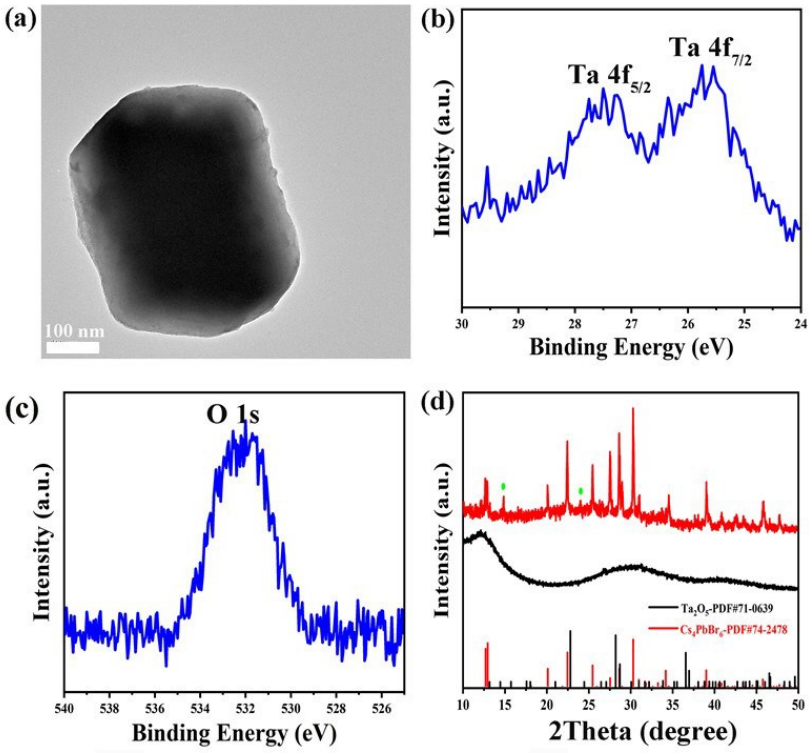

Fig. S5 (a) TEM image of single $Cs_4PbBr_6/CsPbBr_3@Ta_2O_5$ microcrystal, XPS of (b)Ta 4f and (c) O 1s, (d) X-ray diffraction patterns of pure Ta_2O_5 and $Cs_4PbBr_6/CsPbBr_3@Ta_2O_5$ microcrystals.

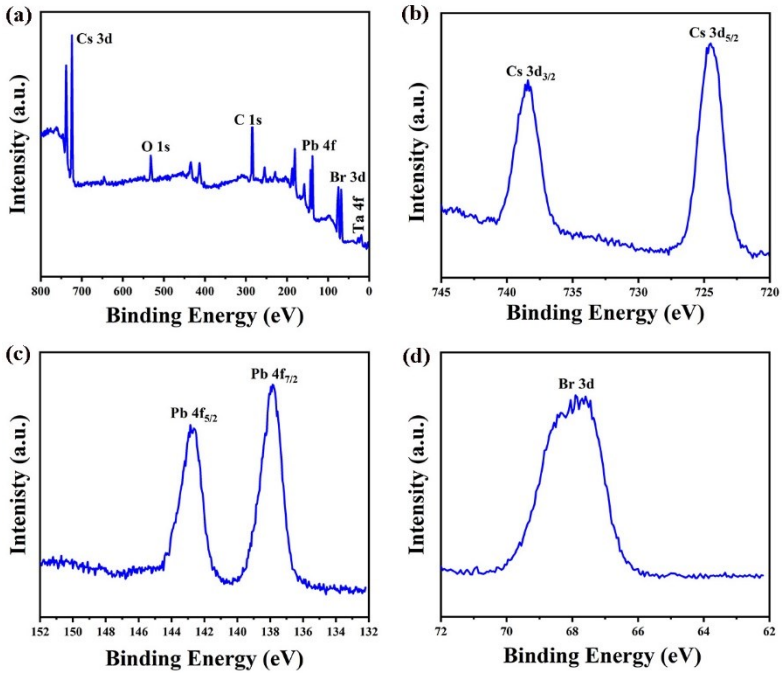

Fig. S6 XPS spectrum of (a) survey, (b) Cs 3d, (c) Pb 4f, (d) Br 3d.

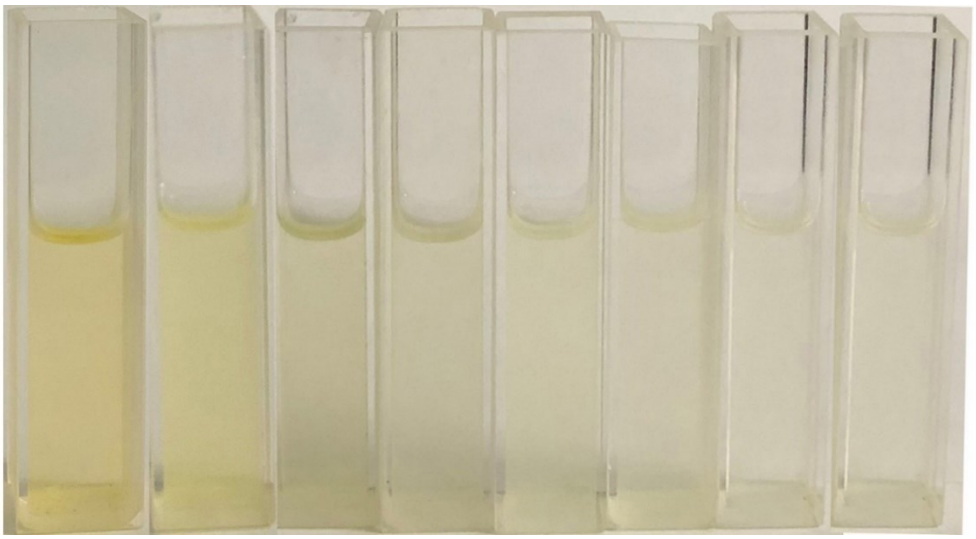

Fig. S7 The photographs corresponding digital images of as-prepared products under day light (From left to right: with the amount of TTEO being increased from 0 to 2, 4, 6, 8, 10, 15 and 20 μL in hexane solution).

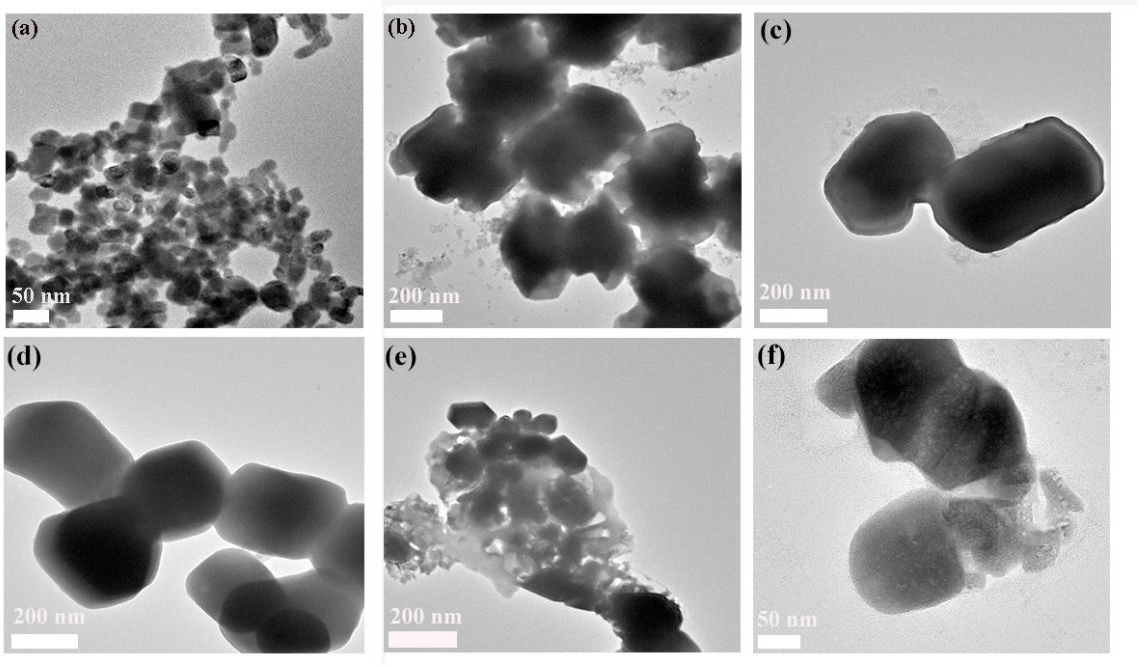

Fig. S8 TEM images of (a) $CsPbBr_3$ NCs, and $Cs_4PbBr_6/CsPbBr_3@Ta_2O_5$ with different amounts of TTEO (b) 2, (c) 6, (d) 10, (e)15 and (f) 20 μL.

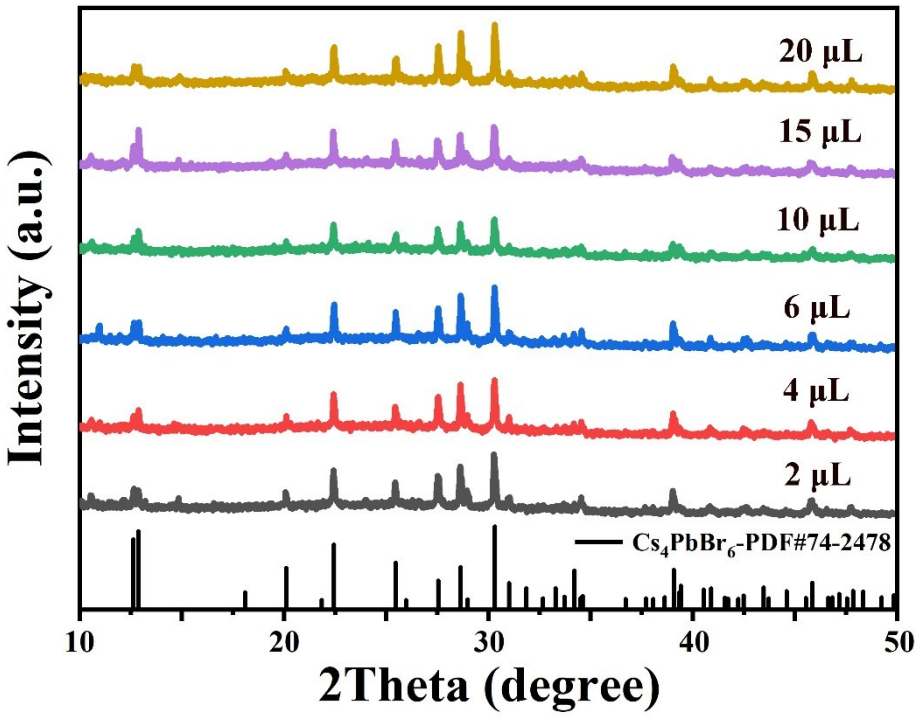

Fig. S9 XRD patterns of $Cs_4PbBr_6/CsPbBr_3@Ta_2O_5$ microcrystals with different amounts of TTEO, as indicated on the frames.

Table S3. PL Lifetime for Janus $Cs_4PbBr_6/CsPbBr_3@Ta_2O_5$ MCs with different amounts of TTEO (PL lifetime is fitted by a biexponential decay function).

TTEO (μL)	τ1 (ns)	τ2 (ns)	A1	A2	τ_{Avg} (ns)	PLQY (%)	Knr
0	2.84	12.53	7.38E+9	151237.1	2.84	2.1	0.34385
2	3.46	19.34	2222.2	746.97	17.96	27.9	0.0401
4	6.38	25.62	7306.11	2622.15	22.78	41.3	0.0258
6	6.15	37.71	2152.74	905.34	35.83	61.0	0.0109
8	8.91	69.43	1752.16	1047.54	67.80	94.7	0.0008
10	7.96	56.43	1967.18	950.61	54.51	71.4	0.0052
15	10.26	56.13	1824.85	1085.60	53.69	30.7	0.0129
20	7.39	41.80	2157.71	817.23	39.17	22.1	0.0199

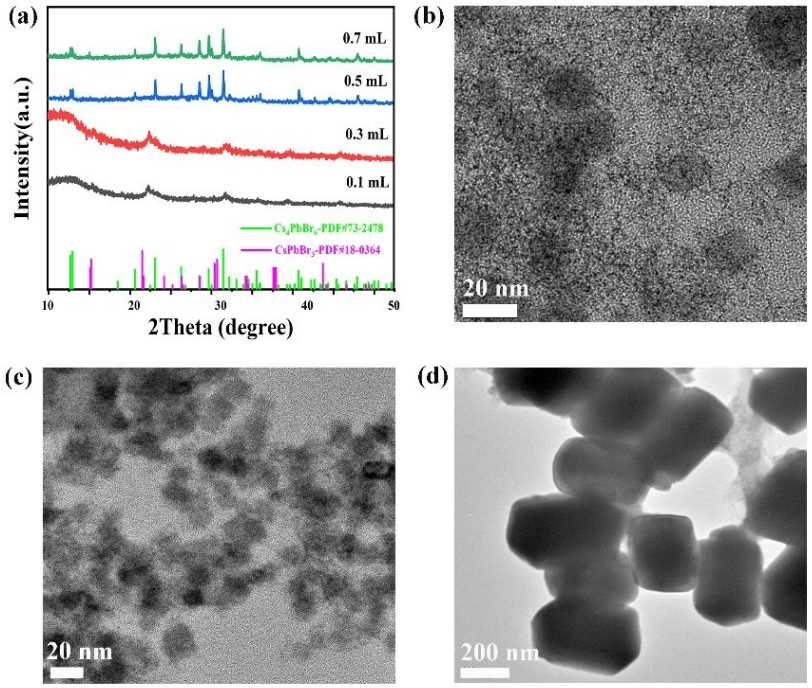

Fig. S10 (a) XRD patterns and TEM images of the product with different amounts of DMF solution adding: (b) 0.1 mL, (c) 0.3 mL, (d) 0.7 mL.

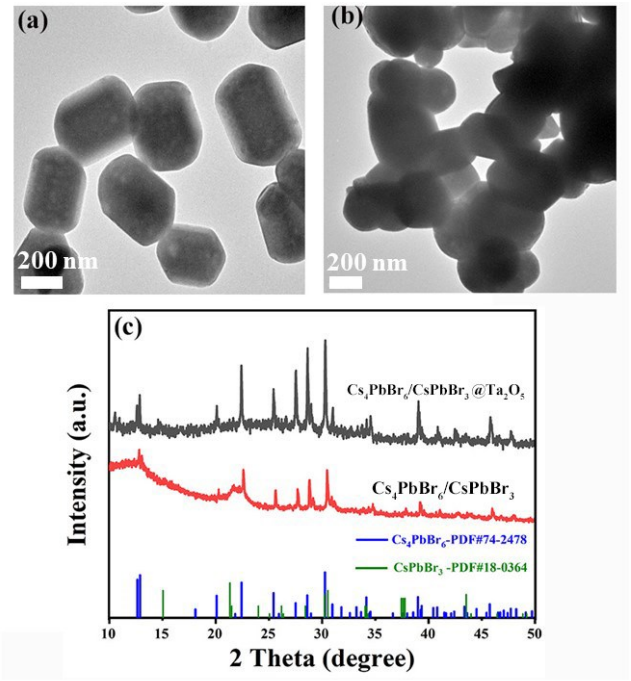

Fig. S11 TEM image of (a) $Cs_4PbBr_6/CsPbBr_3@Ta_2O_5$ and (b) $Cs_4PbBr_6/CsPbBr_3$ after continuous thermal treatment, (c) XRD patterns of $Cs_4PbBr_6/CsPbBr_3@Ta_2O_5$ MCs and $Cs_4PbBr_6/CsPbBr_3$ after continuous thermal treatment, as indicated on the frames.

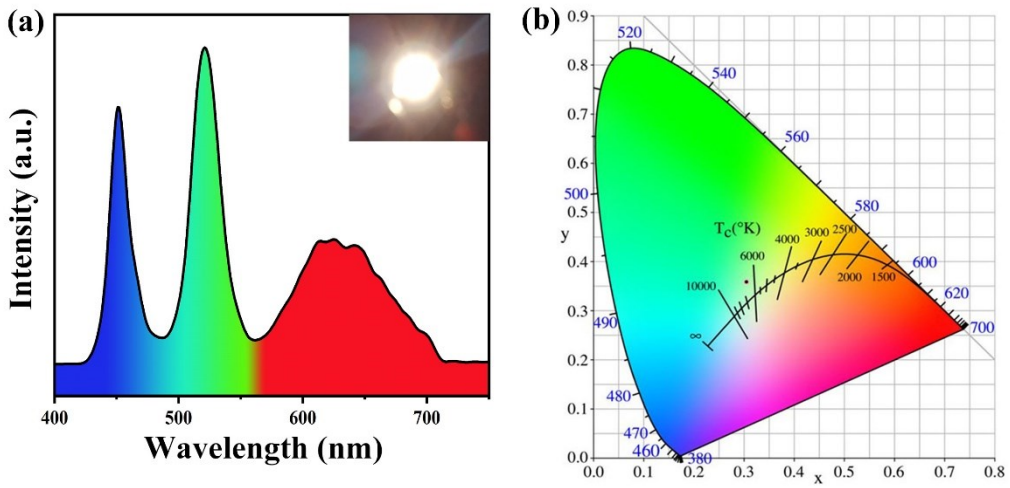

Fig. S12 (a) Emission spectrum of the WLED device fabricated by depositing $Cs_4PbBr_6/CsPbBr_3$ and $CdSe_2$ over blue InGaN chips, inset: photo of the operating WLED. (b) CIE color coordinates of the corresponding WLED device.